Prediction of the energy dependence of molecular fragmentation cross sections for collisions of swift protons with ethane and acetylene

Remigio Cabrera-Trujillo, John R. Sabin, Erik Deumens, and Yngve Öhrn
Departments of Physics and Chemistry, University of Florida, Gainesville, Florida 32611-8435 USA
(Received 25 October 2004; published 22 April 2005)

We report the energy-dependent fragmentation cross sections for several of the more likely fragmentation channels for protons with up to 10 keV impact energy colliding with acetylene and ethane. We find that the predominant channels are those which involve the dissociation of a carbon-hydrogen bond, and we find that the cross sections for these channels are maximum in the low-projectile-energy region. The cross sections for fragmentation involving dissociation of a C-C bond are an order of magnitude smaller and peak at somewhat higher projectile energy. Although there are no experimental values with which to compare, it appears that selection of projectile energy can be used to influence branching ratios in proton-hydrocarbon collisions and, by implication, in other ion-molecule and atom-molecule collisions.

DOI: 10.1103/PhysRevA.71.044702 PACS number(s): 34.50.Lf

The damage to materials caused by projectiles such as electrons, protons, and α particles involves, depending on the system under investigation, the formation of intermediate species, such as radicals, secondary ions, and δ electrons. Via a number of mechanisms, these participate in reactive processes that cause further damage. For charged particles, it is well known that the greatest damage—that is, the largest energy deposition—occurs when projectiles are slowed to kinetic energies comparable to molecular ionization and bond energies. Some projectiles, particularly electrons, can cause great damage, including bond rupture, down to thermal energies.

Understanding the mechanisms for fragmentation of molecular targets by swift ions is important in many fields of study, including radiation therapy, radiation hardening of micro-electronics, and atmospheric chemistry. Some work has been done on fragmentation processes involving charge-induced fragmentation of nucleobases, where multiple ionizations of a single base are caused by distant collisions with slow, highly charged xenon ions [1]. Other studies of fragmentation dynamics involve phenomena such as field-induced ionization by laser light [2]. The fragmentation dynamics of water, methanol, and benzene have been investigated in this manner.

A theoretical treatment of ion-induced fragmentation should be able to treat all accessible fragmentation channels on an equal footing and ideally apply to a wide range of collision energies.

Obviously, a fully nonadiabatic quantum mechanical treatment is not practical when target systems of some complexity are considered: Computational resources become excessive. In this paper we adopt an approach to dynamics that employs a coupled quantum mechanical description of the electrons and nuclei. In this implementation, the nuclear wave functions are reduced to zero width (classical nuclei). This method, called electron nuclear dynamics (END), which is fully nonadiabatic, has been described in some detail in the literature [3–5] and has been applied to several ion-atom [6,7] and ion-molecule reactive collision systems [8,9].

We have chosen to study the fragmentation of acetylene and ethane molecules in collisions with protons at projectile energies from 10 eV to 10 keV. Although these molecules are chemically simple, they present a sufficiently large number of degrees of freedom that the number of possible product channels is substantial and the expected fragmentation processes are far from trivial.

To calculate fragmentation cross sections at a given energy, one needs to determine the dynamics of the collision over an appropriate range of impact parameters and to determine the fragmentation products for each trajectory.

The cross section for collisional fragmentation of a molecular system into a particular set of products labeled by i for projectile energy E_p is designated σ_i, which can be written as an integral over the impact parameter b for all trajectories yielding products of the sort i times the probability P_i that, at a given energy, those products are produced. Thus

$$\sigma_i(E) = 2\pi \int P_i(E_p,b) b db. \tag{1}$$

In this work, we report fragmentation cross sections for protons colliding with acetylene and ethane for low to intermediate energies using a scheme where electron and nuclear dynamics are fully coupled.

Electron-nuclear dynamics has several attributes that make it appropriate for this application: (a) The method provides a time-dependent treatment of all electrons and nuclei. (b) Instantaneous forces are calculated from the Coulombic Hamiltonian. (c) No precalculated potential energy surfaces are needed. (d) Cartesian laboratory coordinates are used, and thus no transformation to internal coordinates is required during the dynamics. (e) The wave function is parametrized in terms of the complex molecular orbital coefficients $z, z*$, average nuclear positions **R**, and momenta **P**, which are the dynamical variables of the problem. (f) The method conserves energy, momentum, and total angular momentum (g) The method makes no assumptions concerning which channels are open or on the topology of the trajectories. The last of these points is the most significant for this work, as it implies that we are not looking for a particular mode of

decomposition, but rather for whatever reaction products that might result from a given set of initial conditions. We do note, however, that in this implementation of the END theory, we do not treat unbound electrons adequately, and so we report results only up to impact energies below the collision-induced ionization limit of the target.

Our approach for analysis of the energy loss and charge transfer processes is based on application of the time-dependent variational principle (TDVP) to the Schrödinger equation, where the wave function is described in a coherent-state representation. As the details of the END method have been reported elsewhere [3–5], we present here only a very brief description of the fundamental features of the theory.

The TDVP requires that the quantum action should be stationary. Therefore, application of the variational principle yields the time-dependent Schrödinger equation when variations of the wave function $|\xi\rangle$ over the entire state space are performed. Variations over a subspace yield the TDVP approximation for the time evolution over that subspace of the Schrödinger equation. We use a parametrization of the wave function in a coherent-state manifold, which leads to a system of Hamilton's equations of motion [4]. The variational wave function $|\xi\rangle$ is a molecular generalized coherent state [10,11] $|\xi\rangle=|\mathbf{z},\mathbf{R},\mathbf{P}\rangle|\mathbf{R},\mathbf{P}\rangle=|z\rangle|\phi\rangle$ where $|z\rangle$ and $|\phi\rangle$ are the coupled electronic and nuclear wave functions, respectively.

The simplest implementation of the END approach employs a single spin-unrestricted electronic determinant written in terms of nonorthogonal spin orbitals φ_i which are in turn expressed in terms of a basis of augmented Gaussian-atomic-type orbitals of rank K with complex coefficients $\{z_{ji}\}$. The Gaussian-type orbitals are centered on the average positions $\mathbf{R}$ of the participating atomic nuclei which are moving with a momentum $\mathbf{P}$. This representation takes into account the momentum of the electrons explicitly through electron translation factors (ETF's) [12].

The nuclear part of the wave function is represented by localized Gaussian functions which, in the narrow wave-packet limit ($w\rightarrow 0$), become classical trajectories $(\mathbf{R}_k,\mathbf{P}_k)$.

Application of the TDVP then yields the dynamical equations which include the nonadiabatic coupling terms between the electrons and nuclei. Solving the set of equations for $\{\mathbf{z},\mathbf{R},\mathbf{P}\}$ as a function of the time t yields the evolving molecular state that describes the processes that take place during the collision.

For the purpose of discussing charge exchange, we make use of the Mulliken population analysis [13] for the projectile and target.

This scheme has been implemented in the ENDYNE program package [14].

Analysis of the collision requires the specification of initial conditions of the system under consideration. In Fig. 1, we show a schematic representation of the projectile-target arrangement for a proton at **A** impinging on a C_2H_6 molecule. The initial projectile velocity is set parallel to the z axis and directed towards the stationary target with an impact parameter b. In the case of atomic projectiles, we need to consider the initial orientations of only the target. The target center of mass is initially placed at the origin of a Cartesian laboratory coordinate system and its orientation is specified by the angles α and β. For the C_2H_6 molecule, we consider

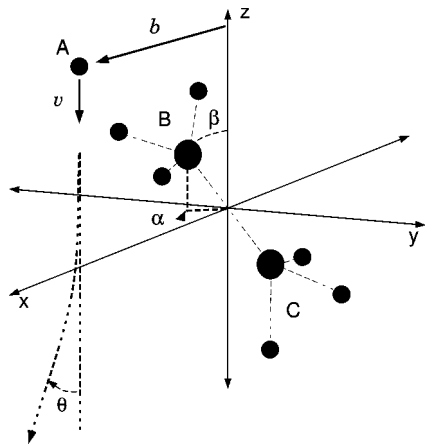

FIG. 1. Schematic representation of the coordinate system used here.

a minimum of three initial orientations of the target with respect to the direction of the incoming beam. These orientations yield a coarse set of grid points for numerical rotational averaging. The three basic target orientations place the molecular bond along the x, y, and z axes. We will label these three orientations I ($\alpha=0$, $\beta=0$), for the molecular C-C bond aligned parallel to the incoming beam; II ($\alpha=0$, $\beta=90$), for the molecular C-C bond perpendicular to the beam, but with the impact parameter measured along the bond; and III ($\alpha=90$, $\beta=90$), for the molecular bond perpendicular to the beam, as well as to the impact parameter direction. We note that orientations I and II require both positive and negative impact parameters on the x axis due to the asymmetry of the CH_3 center where the projectile collides. This provides us with a total of five initial target configurations. We rotationally average to obtain a target property average $\overline{g}$ for a randomly oriented sample. For the particular case of three orientations one obtains

$$\overline{g}=\frac{1}{\pi}[(\pi-2)g_I+(g_{II}+g_{III})], \tag{2}$$

where g_i is the property of interest at orientation i [5].

The electronic basis sets used consists of $[5_s2_p/3_s2_p]$ [15] for hydrogen and $[6_s3_p/3_s2_p]$ for carbon, giving a basis set of rank $K=35$.

In these calculations the protonic projectile is initially set at an distance of 30 a.u. from the target and in the self-consistent (SCF) electronic ground state. If the time it takes for the projectile to reach the target is t_1, then the trajectory is continued until the total time from the start of the trajectory is $t_{tot}=2t_1$ or until there is no further change in the electronic structure of the collision fragments. The impact parameter b is chosen in the range $\{0,20\}$ a.u. in steps of 0.1 from 0.0 to 4.0, of 0.5 from 4.0 to 8.0, and of 1.0 from 8.0 to 20.0. This gives a total of 60 fully dynamical trajectories for each projectile energy.

At the conclusion of each calculated trajectory, one obtains the total system wave function, the nuclear positions and momenta, the charge exchange, and the kinetic energy

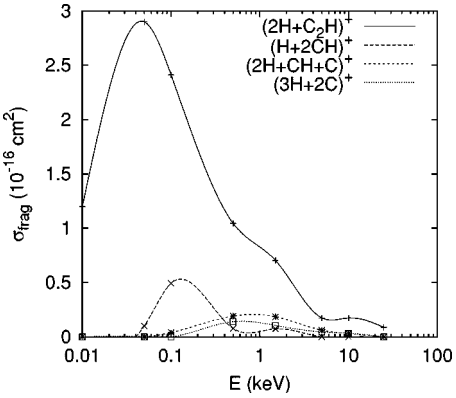

FIG. 2. Energy dependence of the fragmentation cross section for the observed channels for protons colliding with acetylene.

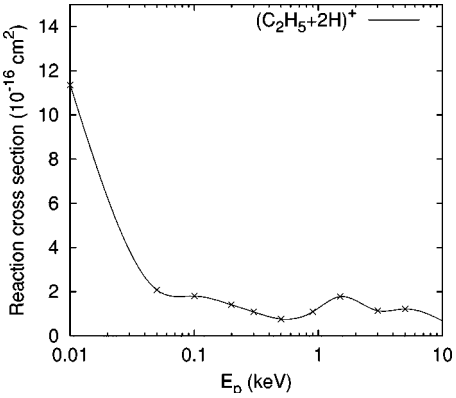

FIG. 3. Energy dependence of the fragmentation cross section for the dominant channel $H^+ \rightarrow C_2H_6 \Rightarrow (C_2H_5+2H)^+$.

loss experienced by the projectile. These quantities yield the fragmentation patterns and fragmentation cross sections for the system.

Acetylene. C_2H_2 is a linear molecule with a strong triple bond; thus high-energy transfer is required between the projectile and the C-C bond to dissociate it. On the other hand, since the bonding energy between a C and a H atoms is smaller, the probability for dissociation of a hydrogen atom from the parent carbon is higher. This is observed in Fig. 2, where we present the total fragmentation cross sections for protons colliding with acetylene as a function of projectile energy. Here, we observe that the largest cross section occurs for the channel $H^+ \rightarrow C_2H_2 \Rightarrow (2H+C_2H)^+$, with a peak around 50 eV. The next group of channels involves dissociation of the C-C bond, where the fragmentation cross section peaks at energies between 100 eV and 1 keV. These channels are $H^+ \rightarrow C_2H_2 \Rightarrow (H+2CH)^+$, $H^+ \rightarrow C_2H_2 \Rightarrow (2H+C+CH)^+$, and $H^+ \rightarrow C_2H_2 \Rightarrow (3H+2C)^+$. Incidentally, the latter two channels have a maximum around the same energy ($\approx$1 keV), since both require energy energy transfer enough to break the C-C and C-H bond.

Note that the product charge is not assigned to any specific fragment. After the collision, Mullikan population analysis [13] is used to identify charges. This procedure gives a probability for finding the excess charge on each of the centers, and since those probabilities are not integral, we indicate only that the charge is distributed quantum mechanically over all the fragments.

Ethane. The channel with the highest cross section is the charge exchange or electron capture channel $H^+ \rightarrow C_2H_6 \Rightarrow (H+C_2H_6)^+$ [9], which has a cross section at $E_p = 10$ eV of approximately 46×10^{-16} cm^2. This compares to the dominant fragmentation cross section, shown in Fig. 3 for $H^+ \rightarrow C_2H_6 \Rightarrow (C_2H_5+2H)^+$, hydrogen atom abstraction combined with charge exchange, of about 11.5×10^{-16} cm^2, nearly an order of magnitude less. The cross section is clearly highest at low impact energy and decays at higher impact energies, with a resonance near $E_p = 2$ keV.

The only other fragmentation patterns with nonvanishing probabilities, which have cross sections again an order of magnitude lower, are presented in Fig. 4.

At 10 eV, the channel with highest cross section is $H^+ \rightarrow C_2H_6 \Rightarrow (C_2H_5+H_2)^+$, similar to the high-cross-section channel $H^+ \rightarrow C_2H_6 \Rightarrow (C_2H_5+2H)^+$, but with a hydrogen molecule formed. The cross section for this channel quickly falls to zero at impact energies over 100 eV.

As the impact energy increases, other fragmentation channels become important, and we see the $H^+ \rightarrow C_2H_6 \Rightarrow (CH_3+CH_3+H)^+$ as well as the $H^+ \rightarrow C_2H_6 \Rightarrow (CH_3+CH_2+2H)^+$ and $H^+ \rightarrow C_2H_6 \Rightarrow (CH_3+C+4H)^+$ channels appearing at impact energies of from 100 eV to 10 keV. These involve dissociation of the C-C bond. Channels requiring specific orientations to occur, such as $H^+ \rightarrow C_2H_6 \Rightarrow (CH_3+CH_4)^+$, have very small cross sections over the entire energy range. We presume this is because such reactions are highly sensitive to the orientational relations of the collision partners, as well as to the energetics of the process. As the total energy and momentum of the system must be conserved in any collision process, it is more difficult to form new chemical bonds in the process than to fragment a projectile or target and carry excess energy away as fragment kinetic energy.

Many of the fragmentation cross section curves shown in Figs. 3 and 4 show some structure. The structure is attributed to a complicated interplay of target orientation, charge exchange, and energetic resonance with the chemical bonds. We have not been able to deconvolute these contributions.

Of the many possible fragments that one might expect from a $H^+ \rightarrow C_nH_m$ collision with projectile energies in the range from 10 eV to 10 keV, which is unrestricted as to tar-

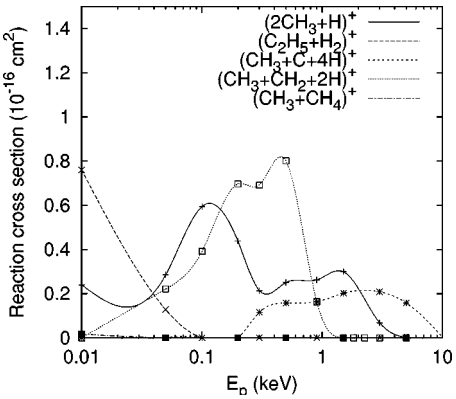

FIG. 4. Energy dependence of the cross sections for the remaining channels observed in the $H^+ \rightarrow C_2H_6$ collision.

get orientation, only a very few are actually found. For example, for collisions of protons with ethane, one might expect that all species such as C_2H_n ($n=0-6,7$), CH_n ($n=0-4,5$), and H_n ($n=1-3$) all could be observed. In addition, each of the fragments could be either neutral or with a positive charge or two. All combinations which satisfy the stoichiometry are possible products. Although the various fragmentation channels are all possible, we note that only a few of them have probabilities large enough to yield a nonvanishing cross section.

From the foregoing, it is evident that product branching ratios for collisions of the sort discussed here can easily be affected by a judicious selection of projectile energy.

In summary, we have studied the fragmentation patterns for the $H^+ \rightarrow C_2H_2$ and C_2H_6 systems over three decades of projectile energy, and we report the energy-dependent fragmentation cross sections for those processes with the largest cross sections. We find that the most likely channel involves dissociation of a C-H bond with a high probability at lower projectile energies followed by the dissociation of the C-C bond at higher projectile energies. The method used in this study does not impose any restrictions on possible trajectories or reaction channels and preserves the conservation laws. It is well suited for studies where the reaction channel is not predetermined.

This work has been supported in part by ONR (Grant No. N0014-96-1-0707 to J.R.S and Grant No. N0014-00-1-0197 to N.Y.Ö.) and by an IBM SUR grant to the Quantum Theory Project. This support is gratefully acknowledged.

[1] J. de Vries, R. Hockstra, R. Morgenstern, and T. Schlathölter, Phys. Rev. Lett. **91**, 053401 (2003).
[2] F. A. Rajgara, M. Krishnamurthy, and D. Mathur, Phys. Rev. A **68**, 023407 (2003).
[3] E. Deumens, A. Diz, H. Taylor, and Y. Öhrn, J. Chem. Phys. **96**, 6820 (1992).
[4] E. Deumens, A. Diz, R. Longo, and Y. Öhrn, Rev. Mod. Phys. **66**, 917 (1994).
[5] D. Jacqemin, J. A. Morales, E. Deumens, and Y. Öhrn, J. Chem. Phys. **107**, 6146 (1997).
[6] R. Cabrera-Trujillo, J. R. Sabin, Y. Öhrn, and E. Deumens, Phys. Rev. A **61**, 032719 (2000).
[7] R. Cabrera-Trujillo, J. R. Sabin, E. Deumens, and Y. Öhrn, Phys. Rev. A **66**, 022706 (2002).
[8] M. Coutinho-Netto, E. Deumens, and Y. Öhrn, J. Chem. Phys. **116**, 2794 (2002).
[9] R. Cabrera-Trujillo, J. R. Sabin, Y. Öhrn, and E. Deumens, J. Electron Spectrosc. Relat. Phenom. **129**, 303 (2003).
[10] D. J. Thouless, Nucl. Phys. **21**, 225 (1960).
[11] J. R. Klauder and B.-S. Skagerstam, *Coherent States, Applications in Physics and Mathematical Physics* (World Scientific, Singapore, 1985).
[12] J. B. Delos, Rev. Mod. Phys. **53**, 287 (1981).
[13] R. S. Mulliken, J. Chem. Phys. **36**, 3428 (1962).
[14] E. Deumens, A. Diz, H. Taylor, J. Orero, B. Mogensen, J. A. Morales, M. C. Neto, R. Cabrera-Trujillo, and D. Jacquemin, computer code ENDYNE, version 2.8, software for electron nuclear dynamics, Quantum Theory Project (QTP), University of Florida, 2000.
[15] D. E. Woon and T. H. Dunning, J. Chem. Phys. **100**, 2975 (1994).